



# Molecular structure and vibrational and chemical shift assignments of 6-(2-hydroxyethyl)-2,3,4-triphenyl-2,6-dihydro-7H-pyrazolo[3,4-d]pyridazin-7-one by DFT and *ab initio* HF calculations

Sibel Demir<sup>a,\*</sup>, Muharrem Dinçer<sup>a</sup>, Emine Şahan<sup>b</sup>, Elif Korkusuz<sup>b</sup>, İsmail Yıldırım<sup>b</sup>

<sup>a</sup> Department of Physics, Faculty of Arts and Sciences, Ondokuz Mayıs University, 55139 Kurupelit, Samsun, Turkey

<sup>b</sup> Department of Chemistry, Faculty of Arts and Sciences, Erciyes University, 38039 Kayseri, Turkey

## ARTICLE INFO

### Article history:

Received 15 July 2010

Received in revised form 1 November 2010

Accepted 1 November 2010

Available online 6 November 2010

### Keywords:

X-ray structure determination

B3LYP

Hartree–Fock

GIAO

<sup>1</sup>H and <sup>13</sup>C NMR and vibrational assignment

AM1 semi-empirical method

## ABSTRACT

The molecular geometry, vibrational frequencies, gauge including atomic orbital (GIAO) <sup>1</sup>H and <sup>13</sup>C chemical shift values and several thermodynamic parameters of 6-(2-hydroxyethyl)-2,3,4-triphenyl-2,6-dihydro-7H-pyrazolo[3,4-d]pyridazin-7-one in the ground state have been calculated by using the Hartree–Fock (HF) and density functional methods (B3LYP) with 6–31G(d) basis set. The results of the optimised molecular structure are presented and compared with the experimental X-ray diffraction. The calculated results show that the optimised geometries can well reproduce the crystal structural parameters and the theoretical vibrational frequencies, and <sup>1</sup>H and <sup>13</sup>C NMR chemical shift values show good agreement with experimental data. The computed vibrational frequencies are used to determine the types of molecular motions associated with each of the experimental bands observed. To determine conformational flexibility, molecular energy profile of the title compound was obtained by semi-empirical (AM1) with respect to selected degree of torsional freedom, which were varied from –180° to +180° in steps of 10°. Besides, molecular electrostatic potential (MEP), frontier molecular orbitals (FMO), and thermodynamic properties were performed at HF and DFT levels of theory.

Crown Copyright © 2010 Published by Elsevier B.V. All rights reserved.

## 1. Introduction

The title compound, is a derivative of 7H-pyrazolo[3,4-d]pyridazin-7-one, which are reported as very important organic compounds because they are widely used as pharmaceuticals and agrochemicals. Their excellent control activities on various plant diseases are studied [1,2]. Pyrazoles are important compounds that have many derivatives with a wide range of interesting properties, such as anti-hyperglycaemic, analgesic, anti-inflammatory, anti-pyretic, anti-bacterial, hypoglycaemic and sedative–hypnotic activity. They were also reported to have non-nucleoside HIV-1 reverse transcriptase inhibitory activity [3,4]. Pyrazolo[3,4-d]pyridazine derivative was obtained from cyclization of 4-benzoyl-1,5-diphenyl-1H-pyrazole-3-carboxylic acid or -acid chloride with 2-hydroxyethyl hydrazine. The title compound is a novel compound synthesized firstly in our laboratories by us. The possible biological properties of the pyrazol, pyridazinone [5,6], and pyrazolo-pyridazinone [7,8] derivatives make it attractive to study these compounds.

In this study, we present results of a detailed investigation of the synthesis and structure characterization of 6-(2-hydroxyethyl)-2,3,4-triphenyl-2,6-dihydro-7H-pyrazolo[3,4-d]pyridazin-7-one using single crystal X-ray, IR, NMR and quantum chemical methods, besides elemental analysis. The geometrical parameters, fundamental frequencies and GIAO <sup>1</sup>H and <sup>13</sup>C NMR chemical shift values of the title compound in the ground state were calculated using the Hartree–Fock (HF) and DFT (B3LYP) methods with the 6–31G(d) basis set. These calculations are valuable for providing insight into molecular parameters and the vibrational and NMR spectra. The aim of this work is to explore the molecular dynamics and the structural parameters that govern the chemical behaviour, and to compare predictions made from theory with experimental observations.

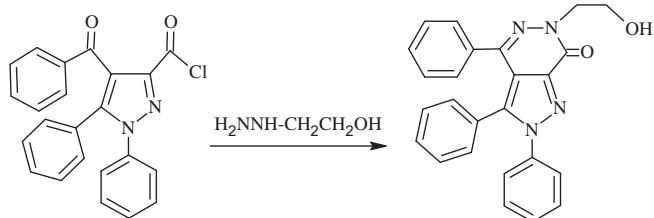
## 2. Experimental

### 2.1. Synthesis

Melting points were measured on an Electrothermal 9200 apparatus and are uncorrected. Microanalysis was performed using a Leco-932 CHNS-O Elemental Analyzer. The <sup>1</sup>H and <sup>13</sup>C NMR spectra were measured with a Bruker Avance III 400 MHz spectrometer and the chemical shifts are expressed in ppm relatively to TMS.

\* Corresponding author. Tel.: +90 03623121919/5260; fax: +90 03624576081.

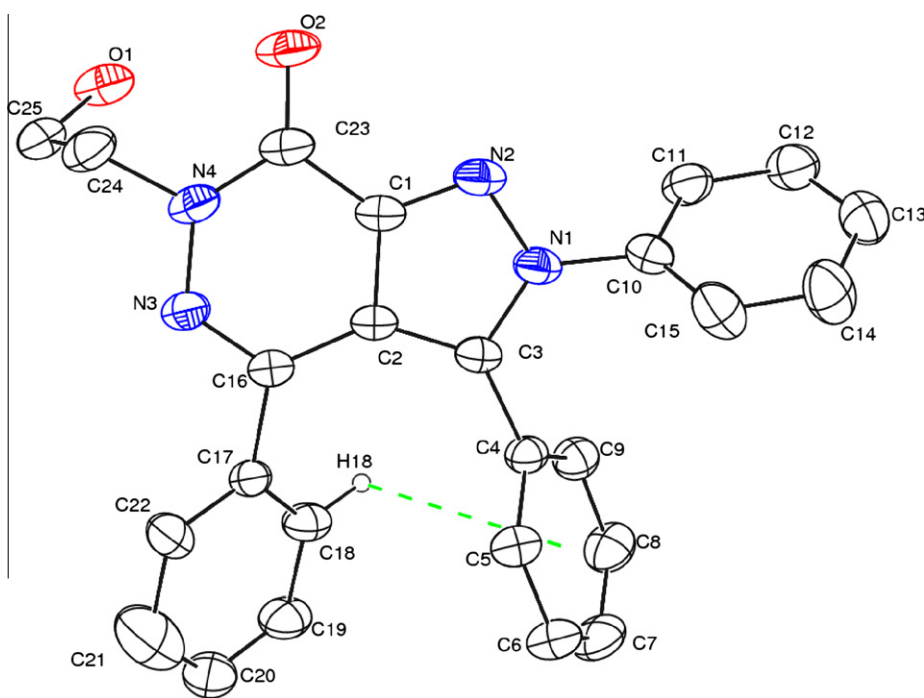
E-mail addresses: [sibeld@omu.edu.tr](mailto:sibeld@omu.edu.tr), [sibdemir@hotmail.com](mailto:sibdemir@hotmail.com) (S. Demir).



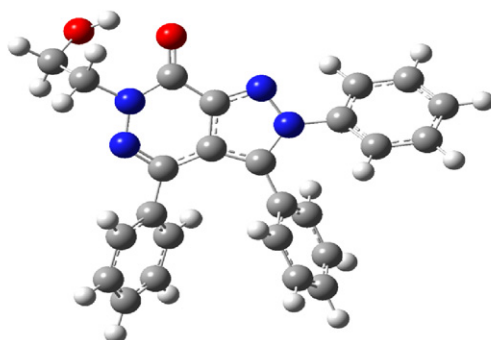
**Scheme 1.** Synthesis scheme of the title compound.

When necessary to identify all C- and H-atoms, complementary NMR experiments (HETCOR, and Exchange with D<sub>2</sub>O) were performed. IR spectra of the compound were recorded in the range of 400–4000 cm<sup>-1</sup> region with a Shimadzu FT-IR 8400 spectrophotometer. Solvents were dried by refluxing with the appropriate drying agents and distilled before use. All other reagents were purchased from Merck, Fluka, Aldrich and used without further purification. The starting material was prepared according to the

literature procedure that described by Ziegler and co-workers [9] and by Akçamur and co-workers [10,11]. The 4-benzoyl-1,5-diphenyl-1H-pyrazole-3-carboxylic acid chloride (0.20 g, 0.52 mmol) and 2-hydroxyethyl hydrazine (0.07 mL, 1.04 mmol) were refluxed in xylene for 5 h. The solvent was evaporated, then the oily residue was treated with diethyl ether and the formed crude product was recrystallized from toluene. (Scheme 1) (yield: 0.16 g, 76%; m.p. 195 °C). IR (ATR,  $\nu$ , cm<sup>-1</sup>): 3460 (O–H), 3065 (aromatic C–H), 2951, 2912 (aliph. C–H), 2000–1750 (overtone or combination bands), 1662 (C=O), 1593–1446 (phenyl, pyridazine and pyrazole rings C–C, C–N), 1225 (C–O). <sup>1</sup>H NMR (400 MHz, CDCl<sub>3</sub>,  $\delta$ , ppm): 7.43–6.85 (m, 15H, ArH), 4.58 (t, 2H, CH<sub>2</sub>–OH), 4.12 (t, 2H, N–CH<sub>2</sub>), 2.73 (b, s, 1H, OH). <sup>13</sup>C NMR (100 MHz, CDCl<sub>3</sub>,  $\delta$ , ppm): 156.86 (C<sub>7</sub>=O), 144.46 (C<sub>7a</sub>), 142.65 (C<sub>4</sub>), 140.16 (C<sub>3</sub>) 138.89 (C<sub>9</sub>), 133.98, 130.43, 129.09, 128.99, 128.89, 128.66, 128.45, 128.16, 127.85, 127.74, 126.03 (arom. C's), 116.68 (C<sub>3a</sub>), 62.41 (CH<sub>2</sub>–OH), 52.80 (N–CH<sub>2</sub>). Analysis calculated for C<sub>25</sub>H<sub>20</sub>N<sub>4</sub>O<sub>2</sub> (408.45 g/mol): C 73.51, H 4.94, N 13.72%; found: C 73.25, H 4.73, N 13.89%.



(a)



(b)

**Fig. 1.** (a) The molecular structure of the title molecule, showing the atom-numbering scheme. Displacement ellipsoids are drawn at the %40 probability level and H atoms are shown as small spheres of arbitrary radii. (b) The theoretical geometric structure of the title compound.

**Table 1**  
Crystallographic data for title compound.

Formula	C <sub>25</sub> H <sub>20</sub> N <sub>4</sub> O <sub>2</sub>
Formula weight	408.45
Temperature (K)	296
Wavelength (Å)	0.71073
Crystal system	Triclinic
Space group	P-1
<i>a</i> (Å)	10.5875(7)
<i>b</i> (Å)	10.6820(7)
<i>c</i> (Å)	11.0305(7)
$\alpha$ (°)	79.701(5)
$\beta$ (°)	69.871(5)
$\gamma$ (°)	62.279(5)
<i>V</i> (Å <sup>3</sup> )	1036.61(11)
<i>Z</i>	2
<i>D</i> <sub>calc</sub> (g/cm <sup>3</sup> )	1.309
<i>F</i> (0 0 0)	428
<i>h, k, l</i> Range	−13 ≤ <i>h</i> ≤ 13 −13 ≤ <i>k</i> ≤ 13 −14 ≤ <i>l</i> ≤ 14
Reflections collected	15,096
Independent reflections	4765
<i>R</i> <sub>int</sub>	0.0347
Reflections observed [ <i>I</i> ≥ 2σ( <i>I</i> )]	3567
<i>R</i> [ <i>I</i> > 2σ( <i>I</i> )]	0.0398
<i>R</i> <sub>w</sub> [ <i>I</i> > 2σ( <i>I</i> )]	0.1036
Goodness-of-fit on Indicator	1.031
Structure determination	Shelxs-97
Refinement	Full matrix
(Δσ) <sub>max</sub> , (Δσ) <sub>min</sub> (e/Å <sup>3</sup> )	0.17, −0.13

**Table 2**  
Hydrogen bonding geometry (Å, °) for the title compound.

D—H...A	D—H	H...A	D...A	D—H...A
O1—H1...O2 <sup>a</sup>	0.93(3)	1.86(3)	2.7856(17)	174(2)
C15—H15...Cg(2)	0.969(19)	2.92(2)	3.736(2)	141.8(14)
C18—H18...Cg(3)	1.010(17)	2.947(17)	3.430(16)	110.2(14)

<sup>a</sup> [−*x*, 1 − *y*, 2 − *z*]; Cg(2): N3—C16; Cg(3): C4—C9.

### 3. Computational details

The molecular structure of the title compound in the ground state (in vacuo) is optimised using Hartree–Fock (HF) and DFT(B3LYP) [12,13] with the 6–31G(d) [14] basis set. For modeling, the initial guess of the Scheme 1. Formation of the title compound was first obtained from the X-ray coordinates. Then, vibrational frequencies for the optimised molecular structures of the title compound were calculated using these methods and then scaled by 0.8929 and 0.9613 [15], respectively. The geometry of the title compound, together with that of tetramethylsilane (TMS), is fully optimised. <sup>1</sup>H and <sup>13</sup>C NMR chemical shifts were calculated within the GIAO approach [16,17] applying the same methods and basis set as used for geometry optimisation. The <sup>1</sup>H and <sup>13</sup>C NMR chemical shifts were converted to the TMS scale by subtracting the calculated absolute chemical shielding of TMS ( $\delta = \Sigma_0 - \Sigma$ , where  $\delta$  is the chemical shift,  $\Sigma$  is the absolute shielding and  $\Sigma_0$  is the absolute shielding of TMS), with values of 32.52 (<sup>1</sup>H) and 199.79 (<sup>13</sup>C) ppm for HF/6–31G(d) and 32.10 (<sup>1</sup>H) and 189.40 (<sup>13</sup>C) ppm for B3LYP/6–31G(d), respectively. All calculations were performed using the GaussView Molecular Visualization program [18] and Gaussian 03 program package [19] on a personal computer without specifying any symmetry for the title molecule. In order to describe conformational flexibility of the title molecule, the selected torsion angle, T(N2–N1–C10–C11) and T(C25–C24–N4–N3), was varied from −180 to 180° in every 10° and the molecular energy profile as a function of the selected torsional degree of freedom is obtained by performing single point

#### 2.1.1. Crystal data for the title compound

CCDC 770493, C<sub>25</sub> H<sub>20</sub> N<sub>4</sub> O<sub>2</sub>, triclinic, space group P-1; *Z* = 2, *a* = 10.5875(7), *b* = 10.682(7), *c* = 11.0305(7) Å,  $\alpha$  = 79.701(5),  $\beta$  = 69.871(5),  $\gamma$  = 62.279(5)°; *V* = 1036.61(11) Å<sup>3</sup>, *F*(0 0 0) = 428, *D*<sub>x</sub> = 1.309 g cm<sup>−3</sup>.

Full crystallographic data are available as supplementary material.

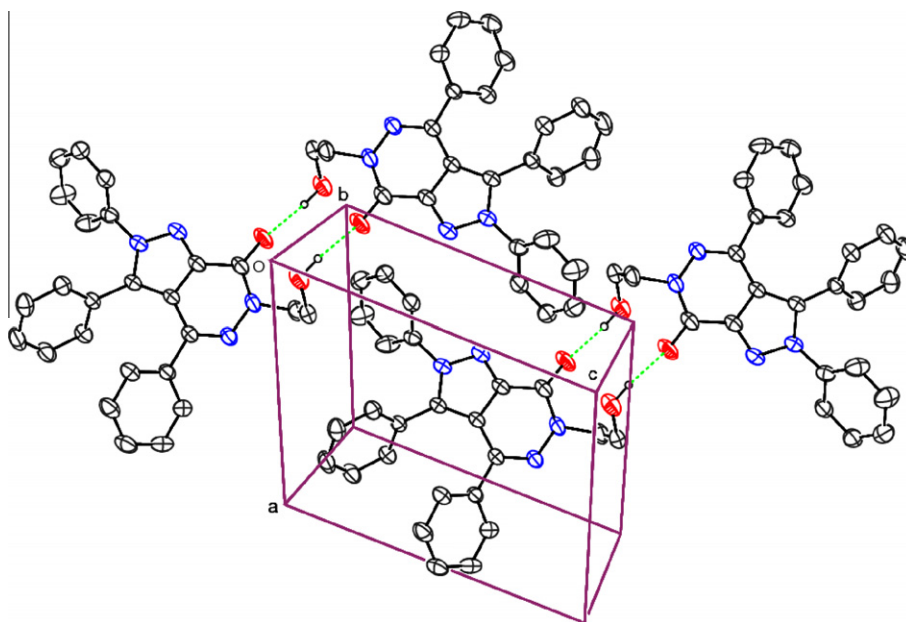


**Fig. 2.** Part of the crystal structure of the title molecule, showing the formation of a chain of centrosymmetric *R* dimers. For the clarity, only H atoms involved in hydrogen bonding have been included.

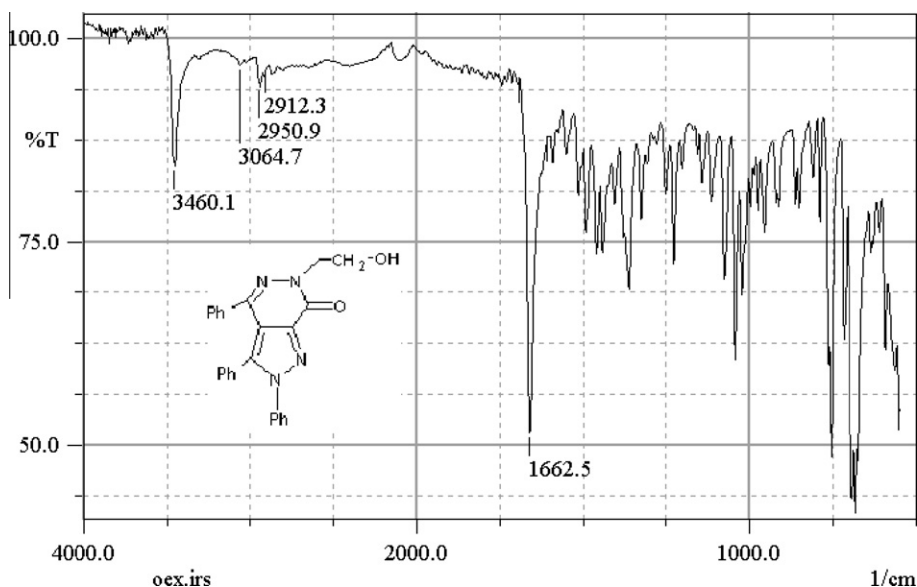


Fig. 3. FT-IR (ATR) spectrum of the title compound.

**Table 3**  
Comparison of the observed and calculated vibrational spectra of the title compound.

Assignments	Experimental IR with ATR (cm <sup>-1</sup> )	Calculated (cm <sup>-1</sup> ) (6–31(d))	
		HF	DFT/B3LYP
$\nu$ O–H (hydroxy ethyl)	3460	3642	3389
$\nu_s$ C–H (phenyl ring)	–	3042– 3030	3123– 3106
$\nu_{as}$ C–H (phenyl ring)	3065	3026– 3016	3103– 3090
$\nu_{as}$ CH <sub>2</sub> (hydroxy ethyl)	2951	2971	3038
$\nu_s$ CH <sub>2</sub> (hydroxy ethyl)	2912	2925– 2837	2979– 2891
$\nu$ C=O + $\beta$ C–C–N	1662	1728	1615
$\nu$ C=N (pyridazin)	1593	1647	1474
$\nu$ C–C (phenyl ring)	–	1620– 1588	1599– 1570
$\nu$ C=C + $\nu$ C=N (pyrazol)	1446	1562	1534
$\alpha$ CH <sub>2</sub>	–	1492/1453	1502
$\beta$ C–H (phenyl ring)	–	1493	1500
$\gamma$ C–H + $\alpha$ CH <sub>2</sub> + $\nu$ C–C–C (pyrazol)	–	1468	1495
$\gamma$ O–H + $\omega$ CH <sub>2</sub>	–	1423– 1373	1401– 1375
$\nu$ C–N–C + $\nu$ C–N–N (pyrazol)	–	1364	1345
$\delta$ CH <sub>2</sub>	–	1342/1247	1355
$\gamma$ CH <sub>2</sub>	–	1307– 1282	1345– 1338
$\beta$ C–N–N (pyrazol + pyridin)	–	1230	1327
$\nu$ N–N (pyrazol ring)	–	1214	–
$\alpha$ C–H	–	1192– 1158	1192– 1176
$\nu$ C–O + $\gamma$ CH <sub>2</sub>	1225	1110/1041	1107
$\delta$ C–H	–	1098–984	997/965
$\theta$ (phenyl ring)	–	973	958
$\theta$ (pyrazol ring)	–	958	958
$\nu$ C–C (hydroxy ethyl)	–	835	941
$\beta$ deformation (pyrazol + pyridin)	782–740	808	806
$\omega$ (phenyl ring)	708–650	805–689	804–701
$\gamma$ O–H	–	370	495

Notes: Vibrational modes:  $\nu$ , stretching;  $s$ , symmetric;  $as$ , asymmetric;  $\alpha$ , scissoring;  $\gamma$ , rocking;  $\omega$ , wagging;  $\delta$ , twisting;  $\theta$ , ring breathing;  $\beta$ , in-plane bending.

calculations on the calculated potential energy surface, and the molecular energy profile was obtained at the AM1 computations.

For the calculations of the MEP [20,21], the same level of theory B3LYP/6–31G(d), were used. The thermodynamic properties of the title compound at different temperatures were calculated on the basis of vibrational analyses, using B3LYP/6–31G(d) level.

## 4. Results and discussion

### 4.1. Crystal structure

The title compound, an Ortep-3 [22] view of which is shown in Fig. 1, crystallises in the triclinic space group P-1 with two molecules in the unit cell, details of which are given in Table 1. The asymmetric unit in the crystal structure contains only one molecule. The title molecule is composed of a hydroxyethyl, triphenyl and dihydropyrazolo pyridazine group.

There are two obviously different C–N bond distances in the pyrazole ring, viz. C1=N2 and C3–N1. The C1=N2 bond length is all longer than and C3–N1 bond length is all shorter than those found in similar structures [C=N 1.291(2)–1.300(10) Å, C–N 1.482(2)–1.515(9) Å] [23], resulting from the conjugation of electrons of atom N with atom C. In this relation, these results are consistent with the respect to the different pyrazole derivatives. Moreover, the N–N bond length (1.356 Å) is shorter than those found in the above-cited structures [N–N 1.373(2)–1.380(8) Å] [24]. In the title compound, six atoms of pyridine ring defines a plane (P). The P is nearly orthogonal to plane the consist of C24, C25 and O1 atoms, with the dihedral angle between them being 80.18 (7)°.

Perspective view of the crystal packing in the unit cell is shown in Fig. 2. In the crystal structure, intermolecular O–H...O hydrogen bonds form centrosymmetric dimers which are linked by further O–H...O hydrogen bonds involving hydroxyethyl molecules (Fig. 2). Hydroxyl atom in the ethyl at (x, y, z) acts as hydrogen-bond donor, via atom H1, to ring atom O2 in the molecule at (–x, 1–y, 2–z), so generating by inversion a centrosymmetric dimer characterized by R<sub>2</sub><sup>2</sup> (14) motif [25] (Fig. 2). There is two C–H...Cg ( $\pi$ -ring) (edge to face) intermolecular interactions, details of which are given in Table 2. Atom C15 at (x, y, z) forms a C–H...Cg ( $\pi$ -ring) contact, via atom H15, with the centroid of the N3–C16 ring [fractional centroid coordinates: 0.3791(5), 0.31887(5), 0.71339(5)] of the molecular at (1–x, 1–y, 1–z). In addition,

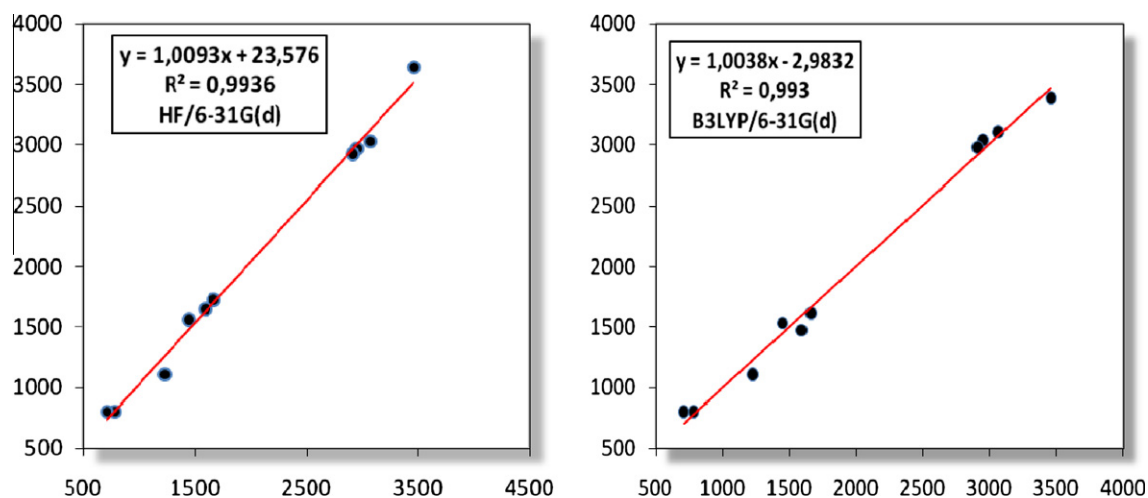


Fig. 4. Correlation graphics of calculated and experimental frequencies of the title compound.

Table 4

Theoretical and experimental  $^{13}\text{C}$  and  $^1\text{H}$  isotropic chemical shifts (with respect to TMS all values in ppm) for the title compound.

Atom	Experimental (CDCl <sub>3</sub> )	Calculated chemical shift (ppm)	
		B3LYP	HF
C1	144.46	136.83	146.79
C2	116.28	109.5	109.71
C3	142.65	129.85	144.42
C4	128.99	123.36	125.01
C5	127.74	118.87	126.69
C6	128.66	111.68	117.83
C7	128.89	110.83	120.35
C8	128.66	113.82	120.18
C9	126.03	119.22	126.86
C10	140.16	132.74	135.52
C11	126.68	112.82	119.59
C12	129.09	114.45	120.49
C13	130.43	111.92	119.74
C14	–	112.64	118.65
C15	126.68	111.6	118.79
C16	138.89	137.26	151.16
C17	–	126.56	128.78
C18	128.16	116.6	124.08
C19	128.45	109.25	114.9
C20	133.98	107.13	115.33
C21	128.45	111.75	118.08
C22	127.85	114.78	122.71
C23	156.86	144.67	158.38
C24	52.86	37.69	35.4
C25	62.41	47.66	43.8
H1	2.73	1.75	0.39
H5	7.38	5.47	5.93
H6	7.12	4.96	5.25
H7	6.82	5.19	5.66
H8	7.10	5.45	6.12
H9	7.36	5.61	6.08
H11	7.23	5.57	5.95
H12	7.04	5.89	6.31
H13	6.83	5.6	6.04
H14	7.03	5.56	5.94
H15	7.22	4.67	5.01
H18	7.30	4.87	5.16
H19	7.18	4.89	5.18
H20	7.13	5	5.46
H21	7.20	4.47	5.05
H22	7.32	5.53	5.97
H24 <sup>a</sup>	4.12	0.945	0.795
H25 <sup>a</sup>	4.58	1.44	1.23

<sup>a</sup> Average.

atom C18 at  $(x, y, z)$  forms a C–H...Cg ( $\pi$ -ring) contact, via atom H18, with the centroid of the C4–C9 ring [fractional centroid coor-

dinates: 0.66406(7) 0.15893(7) 0.22876(6)] of the molecule at  $(x, y, z)$  (Fig. 2). Additional information for the structure determinations are given in Table 2.

#### 4.2. Vibrational spectra

The FT-IR (ATR) spectrum of the title compound is shown in Fig. 3. The vibrational bands assignments have been made by using Gauss-View molecular visualization program [18]. Table 3 presents the calculated vibrational frequencies and their experimentally measured values. We have compared our calculation of the title compound with their experimental results. To make comparison with experiment, we present correlation graphics in Fig. 4 based on the calculations. As we can see from calculation graphic in Fig. 4 experimental fundamentals are in better agreement with scaled fundamentals and are found to have a better correlation for HF than B3LYP. The frequency calculations were carried out at the same level as the respective optimisation process and by analytic evaluation of second derivatives of energy with respect to the nuclear displacement.

It is well known, that the calculated HF and DFT 'raw' or 'non-scale' harmonic frequencies could significantly overestimate experimental values due to lack of electron correlation, insufficient basis sets and anharmonicity.

Most bands observed in infrared spectra of the title compound belong to modes of 6-(2-hydroxyethyl)-2,3,4-triphenyl-2,6-dihydro-7H-pyrazolo[3,4-d]pyridazin-7-one substituents only some of them may be assigned to group ring C–H and C=C/C–C stretching. These bands have been calculated at 3042–3030 (C–H asymmetric), 3026–3016 (C–H symmetric) and 1620–1588  $\text{cm}^{-1}$  (C=C/C–C stretching) for HF level, and 3123–3106, 3103–3090 and 1599–1570  $\text{cm}^{-1}$  for B3LYP level. In the pyrazolo ring, the C=N + C=C and C–N–C + C–N–N stretching are found to be 1562, 1364  $\text{cm}^{-1}$  for HF/6–31G(d) level and 1534, 1345  $\text{cm}^{-1}$  for B3LYP/6–31G(d) level.

Other essential characteristic vibrations of the title compound are C=N (pyridazine ring) and O–H stretching. These modes have been calculated at 1647, 3642  $\text{cm}^{-1}$  with HF/6–31G(d) and 1474, 3389  $\text{cm}^{-1}$  with B3LYP/6–31G(d), these result from different substitute atoms or atom groups in the molecular structure. The other modes can also be seen in Table 3.

#### 4.3. NMR spectra

GIAO  $^1\text{H}$  and  $^{13}\text{C}$  NMR chemical shift calculations were carried out using the HF and B3LYP methods with the 6–31G(d) basis set

for the optimised geometry. The theoretical GIAO  $^{13}\text{C}$  and  $^1\text{H}$  chemical shift values (with respect to TMS) of the title compound are generally compared to the experimental  $^{13}\text{C}$  and  $^1\text{H}$  chemical shift values. The results of these calculations are also shown in Table 4.

The  $^1\text{H}$  NMR chemical shift values (with respect to TMS) have been calculated to be 0.39–6.31 ppm with HF level and 0.945–5.89 ppm with B3LYP level, whereas the experimental results are observed to be 7.38–2.73 ppm. Since experimental  $^1\text{H}$  chemical shift values were not available for individual hydrogen, we present the average values for  $\text{CH}_2$  hydrogen atoms. The two triplet observed at 4.12 and 4.18 ppm are belonged to  $\text{H}_{24}^*$  (C24),  $\text{H}_{25}^*$  (C25) atoms that have been calculated at 0.795 ( $\text{H}_{24}^*$ ) and 1.23 ( $\text{H}_{25}^*$ ) ppm for HF levels, 0.945 ( $\text{H}_{24}^*$ ) and 1.44 ( $\text{H}_{25}^*$ ) ppm for B3LYP levels. The  $-\text{OH}-$  signals of the hydroxyethyl are observed at 2.73 ppm. The  $\text{C}-\text{H}$  signals of phenyl adjacent to the 7*H*-pyrazolo[3,4-*d*]pyridazine are observed at 6.82–7.38, 6.83–7.23, and 7.13–7.32 ppm.

$^{13}\text{C}$  NMR chemical shift values (with respect to TMS) are observed to be 156.86–52.86 ppm range and found to be 158.38–35.4 ppm range by HF level and 144.67–37.69 ppm range by B3LYP. The chemical shift value of C23 atom bounded pyridazine ring are observed as 156.86 ppm, whereas the corresponding values are 144.67 ppm for B3LYP level and 158.38 ppm for HF level. While the two aliphatic  $\text{CH}_2$  (C24 and C25) carbons of belonging to the hydroxyethyl group are observed at 52.86 and 62.41 ppm, respectively. The other calculated chemical shift values can be seen in Table 4.

#### 4.4. Theoretical structures

Selected geometric parameters obtained experimentally and those calculated theoretically using HF and B3LYP with the 6–31G(d) basis set are listed in Table 5. It is well known that DFT optimised bond lengths are usually longer and more accurate than HF, due to the inclusion of electron correlation. However, according to our calculations, the HF method correlates well for the bond length compared with B3LYP method (Table 5). Although the largest difference between experimental and calculated bond lengths is about 0.273 Å for HF and 0.153 Å for B3LYP. The root mean square error (RMSE) is found to be about 0.0681 Å for HF and 0.0685 Å for B3LYP, indicating that the bond lengths obtained by the HF method show the strongest correlation with the experimental values.

When the X-ray structure of the title compound is compared with its optimised counterparts (see Fig. 5), conformational discrepancies are observed between them.

A logical method for globally comparing the structures obtained with the theoretical calculations is by superimposing the molecular skeleton with that obtained from X-ray diffraction, giving a RMSE of 0.174 Å for HF/6–31G(d) and 0.240 Å for B3LYP/6–31G(d) calculations (Fig. 5). Consequently, the HF method correlates well for the geometrical parameters when compared with B3LYP.

#### 4.5. Conformational analysis

Based on HF/6–31G(d) and B3LYP/6–31G(d) optimised geometry, the total energy of the title compound has been calculated by these two methods, which are  $-1325.84085901$  and  $-1333.76262692$  a.u., respectively. In order to define the preferential position of 7*H*-pyrazolo[3,4-*d*]pyridazine system with respect to the 6–2-hydroxyethyl and phenyl ring, a preliminary search of low-energy structures was performed using AM1 computation as a function of the selected torsion angle  $\text{T}(\text{N}2-\text{N}1-\text{C}10-\text{C}11)$  and  $\text{T}(\text{C}25-\text{C}24-\text{N}4-\text{N}3)$ . The respective value of the selected torsion angles are  $165.4(3)$  and  $-72.1^\circ$  in the X-ray structure, whereas the correspond-

ing value in optimised geometries is  $166.180^\circ$  and  $-84.401^\circ$  for HF/6–31G(d) and  $167.396^\circ$  and  $-92.380^\circ$  for B3LYP/6–31G(d).

Molecular energy profiles with respect to rotations about the selected torsion angles are presented in Fig. 6. According to the results, the low energy domains for  $\text{T}(\text{N}2-\text{N}1-\text{C}10-\text{C}11)$  are located at  $-130^\circ$ ,  $-50^\circ$ ,  $40^\circ$  and  $130^\circ$  having energy of 2.03377, 2.03323, 2.03396 and 2.03302 a.u., respectively, while they are located at  $-70^\circ$  and  $80^\circ$  having energy of 0.20562 and 0.20512 a.u., respectively, for  $\text{T}(\text{C}25-\text{C}24-\text{N}4-\text{N}3)$ . The energy difference between the most favourable and most unfavourable conformers, which arises from the rotational potential barrier calculated with respect to the selected torsion angle is calculated as 0.03766 a.u. for  $\text{T}(\text{N}2-\text{N}1-\text{C}10-\text{C}11)$  and as 0.00127 a.u. for  $\text{T}(\text{C}25-\text{C}24-$

**Table 5**

Selected optimised and experimental geometries parameters of the title compound in ground state.

Parameters	Experimental	Calculated	
		HF 6–31G(d)	DFT/B3LYP 6–31G(d)
<i>Bond lengths (Å)</i>			
C(25)–O(1)	1.402(4)	1.308	1.446
C(24)–N(4)	1.467(3)	1.194	1.476
C(25)–C(24)	1.472(4)	1.483	1.531
N(4)–C(23)	1.343(4)	1.300	1.398
C(23)–C(1)	1.347(3)	1.323	1.448
C(1)–C(2)	1.376(4)	1.360	1.428
C(2)–C(16)	1.375(4)	1.370	1.446
C(16)–N(3)	1.404(4)	1.415	1.321
C(16)–C(17)	1.501(4)	1.500	1.485
C(17)–C(22)	1.479(4)	1.496	1.407
C(22)–C(21)	1.388(4)	1.388	1.397
C(21)–C(20)	1.383(5)	1.386	1.400
C(20)–C(19)	1.367(5)	1.383	1.399
C(19)–C(18)	1.376(5)	1.388	1.398
C(18)–C(17)	1.366(5)	1.381	1.406
C(1)–N(2)	1.394(4)	1.392	1.341
N(2)–N(1)	1.224(3)	1.196	1.377
N(1)–C(3)	1.464(4)	1.484	1.388
C(3)–C(2)	1.381(5)	1.392	1.408
C(3)–C(4)	1.392(6)	1.382	1.476
C(4)–C(9)	1.392(7)	1.386	1.408
C(9)–C(8)	1.332(7)	1.384	1.397
C(8)–C(7)	1.367(6)	1.386	1.400
C(7)–C(6)	1.385(5)	1.390	1.400
C(6)–C(5)	1.441(4)	1.426	1.398
C(5)–C(4)	1.383(4)	1.390	1.407
N(1)–C(10)	1.372(4)	1.375	1.436
C(10)–C(11)	1.383(5)	1.394	1.401
C(11)–C(12)	1.389(4)	1.385	1.397
C(12)–C(13)	1.379(4)	1.389	1.400
C(13)–C(14)	1.372(4)	1.377	1.400
C(14)–C(15)	1.370(3)	1.345	1.398
C(15)–C(10)	1.427(5)	1.400	1.400
RMSE <sup>a</sup>		0.0681	0.0685
Max. difference <sup>a</sup>		0.273	0.153
<i>Bond angles (°)</i>			
O(1)–C(25)–C(24)	112.5(2)	112.237	113.786
O(2)–C(3)–C(1)	106.1(2)	106.132	126.586
N(2)–N(1)–C(10)	105.2(2)	104.196	117.221
N(1)–C(3)–C(4)	111.8(2)	111.377	122.958
N(3)–C(16)–C(17)	120.9(3)	122.193	114.667
N(3)–N(4)–C(24)	119.5(2)	118.465	114.455
C(2)–C(16)–C(17)	127.9(2)	129.256	125.450
C(3)–C(2)–C(16)	119.7(3)	119.803	136.799
C(10)–N(1)–N(3)	112.5(2)	114.150	129.457
RMSE <sup>a</sup>		0.975	12.204
Max. difference <sup>a</sup>		1.65	20.486
<i>Torsion angles (°)</i>			
C(11)–C(10)–N(2)–N(1)	165.4(3)	166.180	167.396
N(2)–C(1)–C(23)–N(4)	118.1(4)	113.543	118.756

<sup>a</sup> RMSE and maximum differences between the bond lengths and angles computed using theoretical methods and those obtained from X-ray diffraction.

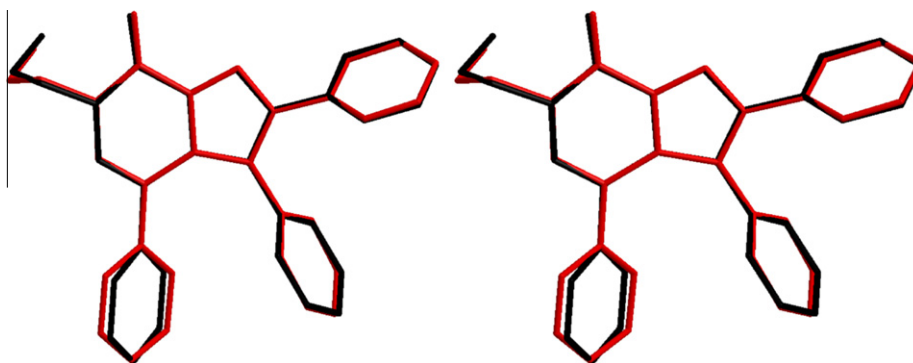


**Fig. 5.** Atom-by-atom superimposition of the structures calculated (black) (A = HF/6-31G(d), B = B3LYP/6-31G(d)) on the X-ray structure (red) of the title compound hydrogen atoms have been omitted for clarity. (For interpretation of the references to colour in this figure legend, the reader is referred to the web version of this article.)

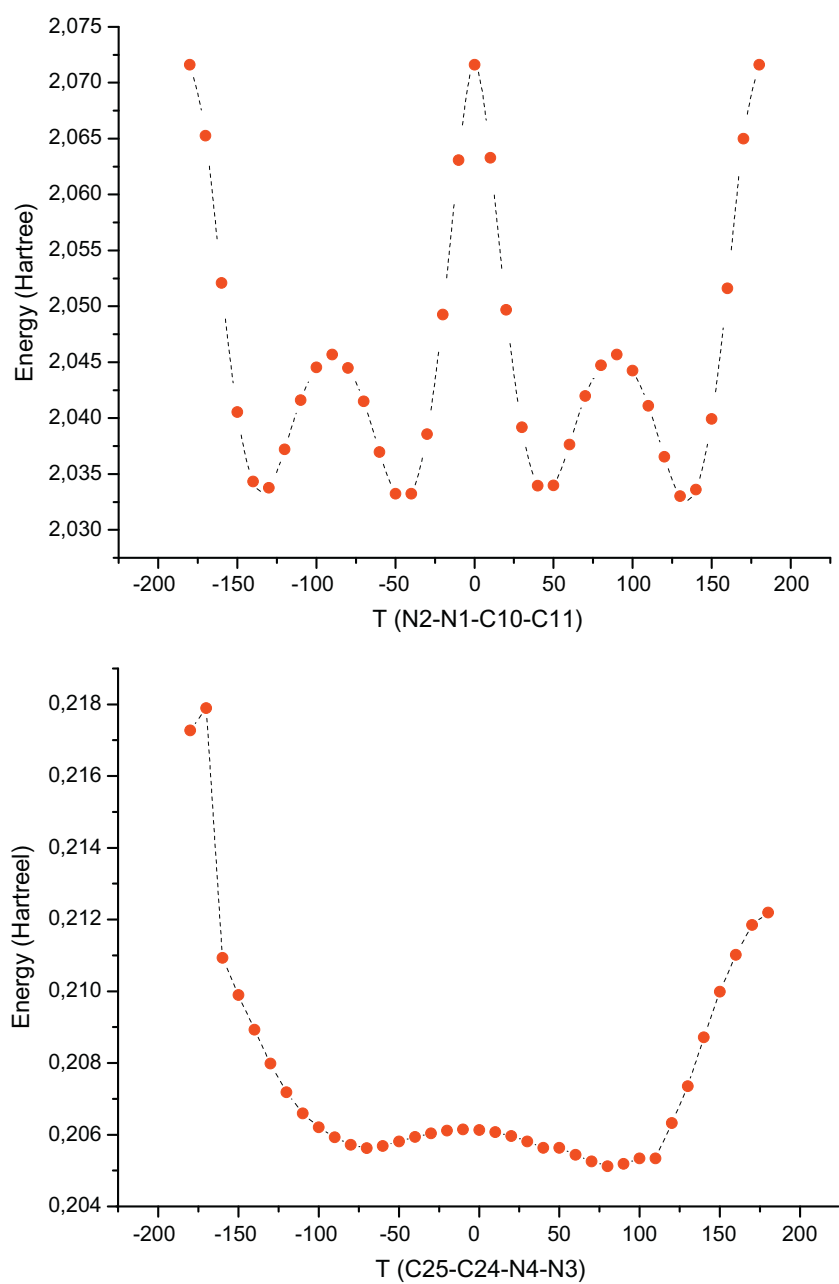


**Fig. 6.** Molecular energy profile of the optimised counterpart of the title compound versus selected degrees of torsional freedom.

N4–N3), when both selected degrees of torsional freedom are considered.

The molecular energy can be divided into bonded and non-bonded contributions. The bonded energy is considered to be independent of torsional angle changes and therefore vanished when relative conformer energies are calculated. The non-bonded energy

is further separated into torsional steric and electrostatic terms [18]. Since the title compound contains no intramolecular hydrogen bond, it can be deduced from the computational results that the most stable conformer of the title compound is principally determined by the non-bonded torsional energy term affected by packing of the molecules.

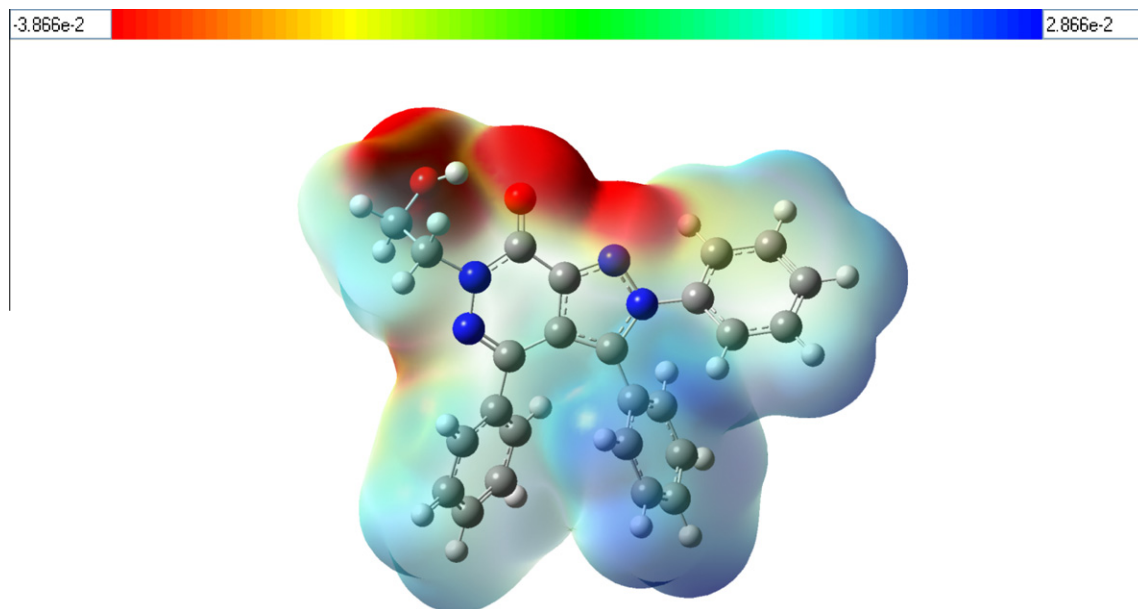


Fig. 7. Molecular electrostatic potential map calculated at B3LYP/6–31G(d) level.

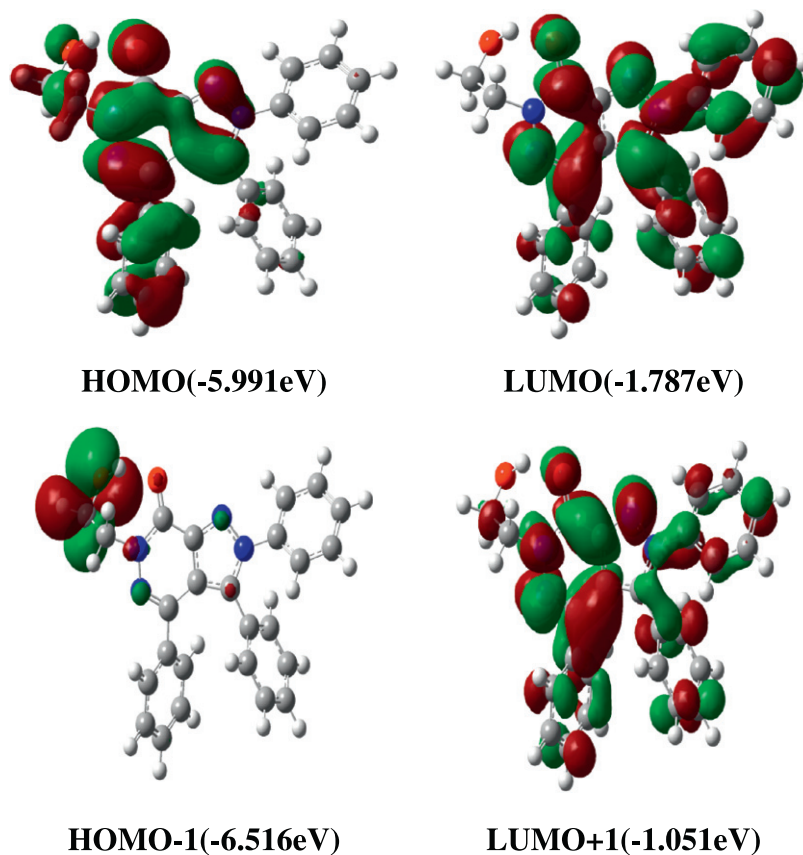


Fig. 8. Molecular orbital surfaces and energy levels given in parentheses for the HOMO-1, HOMO, LUMO and LUMO + 1 of the title compound computed at B3LYP/6–31G(d) level.

#### 4.6. Molecular electrostatic potential

The molecular electrostatic potential,  $V(r)$ , at a given point  $r$  ( $x, y, z$ ) in the vicinity of a molecule, is defined in terms of the interaction energy between the electrical charge generated from the molecule electrons and nuclei and a positive test charge (a proton) located at  $r$ . For the system studied, the  $V(r)$  values were calculated as described previously using the equation [26]:

$$V(r) = \sum Z_A / |R_A - r| - \int \rho(r') / |r' - r| d^3r'$$

where  $Z_A$  is the charge of nucleus  $A$  located at  $R_A$ ,  $\rho(r')$  is the electronic density function of the molecule, and  $r'$  is the dummy integration variable.

The molecular electrostatic potential (MEP) is related to the electronic density and is a very useful descriptor for determining sites for electrophilic attack and nucleophilic reactions as well as hydrogen-bonding interactions [27,28]. The electrostatic potential  $V(r)$  is also well suited for analysing processes based on the 'recognition' of one molecule by another, as in drug-receptor and enzyme-substrate interactions, because it is through their potentials that the two species first 'see' each other [29,30]. Being a real physical property,  $V(r)$  can be determined experimentally by diffraction or by computational methods [31].

To predict reactive sites for electrophilic and nucleophilic attack for the title molecule, MEP was calculated at the B3LYP/6–31G(d) optimised geometry. The negative (red<sup>1</sup>) regions of MEP were related to electrophilic reactivity and the positive (blue) regions to nucleophilic reactivity shown in Fig. 7. As easily can be seen in Fig. 7 this molecule has two possible sites for electrophilic attack. The negative regions are mainly over the O1 and O2 atoms. For the title compound, negative regions were calculated: the MEP value around O2 is more negative than that of O1. These results provide information concerning the region where the compound can interact intermolecularly and metallic bonding. Therefore, Fig. 7 confirms the existence of an intermolecular O–H...O interaction between the protonated and unprotonated O atoms of the hydroxy ethyl and pyridazine.

#### 4.7. Frontier molecular orbitals analysis

The frontier molecular orbitals play an important role in the electric and optical properties, as well as in UV–Vis spectra and chemical reactions [32]. Fig. 8 shows the distributions and energy levels of the HOMO–1, HOMO, LUMO and LUMO + 1 orbitals computed at the B3LYP/6–31G(d) level for the title compound. As can be seen from the figure, both the highest occupied molecular orbital (HOMO) and the lowest-lying unoccupied molecular orbital (LUMO) are mainly delocalised among all the atoms. Both the highest occupied molecular orbitals (HOMOs) and the lowest-lying unoccupied molecular orbitals (LUMOs) are mainly located at the rings and mostly the  $\pi$ -antibonding type orbitals. The value of the energy separation between the HOMO and LUMO is 4.204 eV and this energy gap indicates that the title structure is very stable.

#### 4.8. Thermodynamic properties

Several thermodynamic parameters have been calculated using HF and B3LYP with 6–31G(d) basis set. Table 6 demonstrates thermodynamic parameters of the title compound without of results of experimental.

Besides, based on the vibrational analysis at the B3LYP/6–31G(d) level and statistical thermodynamics, the standard statisti-

**Table 6**

Calculated energies (a.u.), zero-point vibrational energies (kcal mol<sup>-1</sup>), rotational constants (GHz), entropies (cal mol<sup>-1</sup> K<sup>-1</sup>) and dipole moment (D) of the title compound.

Parameters	HF 6–31G(d)	B3LYP 6–31G(d)
Dipole moment (D)	7.888	8.8258
Zero-point vibrational energy kcal mol <sup>-1</sup> )	272.50275	255.17343
Total energy (a.u.)	–1325.84085	–1333.76262
Rotational constants	0.18130 0.13279 0.08312	0.17630 0.13022 0.08012
<i>Entropy (cal mol<sup>-1</sup> K<sup>-1</sup>)</i>		
Rotational	36.328	36.412
Translational	43.911	43.911
Vibrational	87.225	92.409
Total	167.463	172.731

**Table 7**

Thermodynamic properties of the title compound at different temperatures at the B3LYP/6–31G(d) level.

T (K)	$C_{p,m}^0$ (cal mol <sup>-1</sup> K <sup>-1</sup> )	$S_m^0$ (cal mol <sup>-1</sup> K <sup>-1</sup> )	$\Delta H_m^0$ (kcal mol <sup>-1</sup> )
100.00	36.468	98.273	2.237
200.00	53.152	109.867	5.395
298.15	96.145	172.731	15.290
300.00	98.140	173.123	15.624
400.00	107.002	165.285	21.367
500.00	127.750	191.923	32.880
600.00	176.984	269.171	46.166
700.00	194.124	298.094	74.967
800.00	208.029	325.220	94.512

cal thermodynamic functions  $i$ , Standard heat capacities ( $C_{p,m}^0$ ), standard entropies ( $S_m^0$ ), and standard enthalpy changes ( $\Delta H_m^0$  ( $0 \rightarrow T$ )) were obtained and are listed in Table 7. The scale factor for the frequencies is 0.9613, which is a typical value for the B3LYP/6–31G(d) level of calculations. As can be seen from Table 7, the standard heat capacities, entropies and enthalpy changes increase at any temperature from 100.00 to 800.00 K, since increasing the temperature causes an increase in the intensity of the molecular vibration.

For the title compound, the correlation equations between these thermodynamic properties and temperature  $T$ , which can be used for further studies of the title compound, are as follows:

$$C_{p,m}^0 = 15.995 + 0.2276T + 1.5742T^2 (R^2 = 0,9634)$$

$$S_m^0 = 91.09 + 0.128T + 2.03003 \times 10^{-4}T^2 (R^2 = 0,96119)$$

$$H_m^0 = 4.83033 - 0.02696T + 1.73829 \times 10^{-4}T^2 (R^2 = 0,9889)$$

## 5. Conclusions

In this study, we have synthesized a novel compound 7H-pyrazolo[3,4-*d*]pyridazin-7-one derivative, C<sub>25</sub>H<sub>20</sub>N<sub>4</sub>O<sub>2</sub>, and characterized by spectroscopic (FT-IR, NMR) and structural (XRD) techniques as well as microanalysis. To fit the theoretical frequency results with experimental ones for HF and B3LYP levels, we have multiplied the data. Multiplication factors results gained seemed to be in a good agreement with experimental ones. The X-ray structure is found to be very slightly different from its optimised counterparts, and the crystal structure is stabilised by a C–H...O and O–H...O type hydrogen bonds. The results of the HF method show a better fit to experimental values than B3LYP in evaluating

<sup>1</sup> For interpretation of color in Fig. 7, the reader is referred to the web version of this article.

geometrical parameters. It is noted here that the experimental results are for the solid phase and the theoretical calculations are for the gaseous phase. The geometry of the solid state structure is subject to intermolecular forces, such as van der Waals interactions and crystal packing forces. The calculated MEP map agrees well with the solid-state interactions. More commonly, however, the NMR spectrum is used in conjunction with other forms of spectroscopy and chemical analysis to determinate the structures of complicated organic molecules. The correlations between the thermodynamic properties  $C_{p,m}^0$ ,  $S_m^0$  ve  $H_m^0$  and temperatures  $T$  are also obtained.

### Acknowledgement

This study was supported financially by the Research Centre of Ondokuz Mayıs University (Project No: F-461).

### References

- [1] S. Ohuchi, S. Okada, CA 130, 120912, JP 10338589, 1998.
- [2] Y. Yoshikawa, K. Tomiya, T. Kitajima, H. Katsuta, O. Takahashi, S. Inami, Y. Yanase, N. Tomura, J. Kishi, H. Kawasima, CA 129, 16051, EP 841336, 1998.
- [3] S.P. Sing, D. Kumar, Depart. Chem. Heterocycles 31 (1990) 855–860, doi:10.3987/COM-90-5325.
- [4] M.J. Genoin, C. Biles, B.J. Keiser, S.M. Poppe, S.M. Swaney, W.G. Tarpley, Y. Yagi, D.L. Romero, J. Med. Chem. 43 (2000) 1034.
- [5] Li C. Sing, C. Brideau, C.C. Chan, C. Savoie, D. Claveau, S. Charleson, R. Gordon, G. Greig, J.Y. Gauthier, C.K. Lau, Bioorg. Med. Chem. Lett. 13 (2003) 597–600.
- [6] E. Sotelo, N. Fraiz, M. Yanez, R. Laguna, E. Cano, J. Brea, E. Ravina, Bioorg. Med. Chem. Lett. 12 (2002) 1575–1577.
- [7] E. Akbaş, I. Berber, Eur. J. Med. Chem. 40 (2005) 401–405.
- [8] I. Bildirici, A. Şener, I. Tozlu, Med. Chem. Res. 16 (2007) 418–426, doi:10.1007/s00044-007-9082-z.
- [9] E. Ziegler, M. Eder, C. Beleggratis, E. Prewedourakis, Monatsh Chem/Chem Montly 98 (1967) 2249–2251, doi:10.1007/BF00902421.
- [10] Y. Akçamur, G. Penn, E. Ziegler, H. Sterk, G. Kollenz, K. Peters, E.M. Peters, H.G. von Schnering, Organische Chemie Und Biochemie. Monatsh Chem/Chem Montly 117 (1986) 231–245, doi:10.1007/BF00809443.
- [11] M. Dinçer, N. Özdemir, I. Yıldırım, E. Demir, Y. Akçamur, Ş. Işık, Acta Cryst. E60 (2004) o807–o809.
- [12] C. Lee, W. Yang, R.G. Parr, Phys. Rev. B 37 (1988) 785.
- [13] A.D. Becke, J. Chem. Phys. 98 (1993) 5648.
- [14] R. Ditchfield, W.J. Hehre, J.A. Pople, J. Chem. Phys. 54 (1971) 724.
- [15] J.B. Foresman, A. Frisch, Exploring Chemistry with Electronic Structure Methods, second ed., Gaussian Inc., Pittsburgh, PA, 1996.
- [16] R. Ditchfield, J. Chem. Phys. 56 (1972) 5688.
- [17] K. Wolinski, J.F. Hinton, P. Pulay, J. Am. Chem. Soc. 112 (1990) 8251.
- [18] R. Dennington II, T. Keith, J. Millam, GaussView, Version 4.1.2, Semichem, Inc., Shawnee Mission, KS, 2007.
- [19] M.J. Frisch, G.W. Trucks, H.B. Schlegel, G.E. Scuseria, M.A. Robb, J.R. Cheeseman, J.A. Montgomery Jr, T. Vreven, K.N. Kudin, J.C. Burant, J.M. Millam, S.S. Iyengar, J. Tomasi, V. Barone, B. Mennucci, M. Cossi, G. Scalmani, N. Rega, G.A. Petersson, H. Nakatsuji, M. Hada, M. Ehara, K. Toyota, R. Fukuda, J. Hasegawa, M. Ishida, T. Nakajima, Y. Honda, O. Kitao, H. Nakai, M. Klene, X. Li, J.E. Knox, H.P. Hratchian, J.B. Cross, V. Bakken, C. Adamo, J. Jaramillo, R. Gomperts, R.E. Stratmann, O. Yazyev, A.J. Austin, R. Cammi, C. Pomelli, J.W. Ochterski, P.Y. Ayala, K. Morokuma, G.A. Voth, P. Salvador, J.J. Dannenberg, V.G. Zakrzewski, S. Dapprich, A.D. Daniels, M.C. Strain, O. Farkas, D.K. Malick, A.D. Rabuck, K. Raghavachari, J.B. Foresman, J.V. Ortiz, Q. Cui, A.G. Baboul, S. Clifford, J. Cioslowski, B.B. Stefanov, G. Liu, A. Liashenko, P. Piskorz, I. Komaromi, R.L. Martin, D.J. Fox, T. Keith, M.A. Al-Laham, C.Y. Peng, A. Nanayakkara, M. Challacombe, P.M.W. Gill, B. Johnson, W. Chen, M.W. Wong, C. Gonzalez, J.A. Pople, Gaussian 03, Revision E.01, Gaussian, Inc., Wallingford, CT, 2004.
- [20] P. Politzer, S.J. Landry, T. Warnheim, Phys. Chem. 86 (1982) 4767, doi:10.1021/j100221a024.
- [21] J.S. Murray, P. Lane, T. Brinck, P. Politzer, P. Sjöberg, J. Phys. Chem. 95 (1991) 14.
- [22] L.J. Farrugia, J. Appl. Crystallogr. 30 (1997) 565.
- [23] J. Casanovas, A.M. Namba, S. Leon, G.L.B. Aquino, G.V.J. Da Silva, C. Aleman, J. Org. Chem. 66 (2001) 3775.
- [24] C.J. Fahrni, L.C. Yang, VanDerveer, J. Am. Chem. Soc. 125 (2003) 3799.
- [25] J. Bernstein, R.E. Davis, L. Shimon, Chang N.-L. Angew. Chem. Int. Ed. Engl. 34 (1995) 1555.
- [26] P. Politzer, J.S. Murray, Theor. Chem. Acc. (2002) 108–134.
- [27] E. Scrocco, J. Tomasi, Adv. Quant. Chem. (1979) 11–115.
- [28] N. Okulik, A.H. Jubert, Internet Electron. J. Mol. Des. (2005) 4–17.
- [29] P. Politzer, P.R. Laurence, K. Jayasuriya, in: J. McKinney (Ed.), Structure Activity Correlation in Mechanism Studies and Predictive Toxicology, Special Issue of Environ. Health Perspect., 2005, pp. 61–191.
- [30] E. Scrocco, J. Tomasi, Topics in Current Chemistry, vol. 7, Springer, Berlin, 1973, pp. 95–170.
- [31] P. Politzer, D.G. Truhlar, Chemical Applications of Atomic and Molecular Electrostatic Potentials, Plenum Press, New York, 1981. pp. 1–6.
- [32] I. Fleming, Frontier Orbitals and Organic Chemical Reactions, Wiley, London, 1973.